PROCEEDINGS, 43rd Workshop on Geothermal Reservoir Engineering
Stanford University, Stanford, California, February 12-14, 2018
SGP-TR-213

Evolution of Reservoir Tracer Pathways during Multiple Phases of Exploitation

Lara Owens[1], Ben Delwiche[1], John Akerley[1], Peter Rose[2] and Michael Mella[2]

[1]Ormat Nevada Inc, 6225 Neil Road, Reno NV, 89511

[2]Energy & Geoscience Institute, 423 Wakara Way suite 300, Salt Lake City, UT 84108

lowens@ormat.com

Keywords: Nevada, Basin and Range, Tracers, Don Campbell, McGinness Hills

ABSTRACT

Recurring tracer studies from two recently commissioned binary plants are investigated to quantify the evolution in fracture and matrix pathways throughout a highly permeable reservoir. Ormat implemented tracer tests within the first year of operation using several unique naphthalene sulfonate tracers and again during the third year following the start-up of a second phase of operation, effectively doubling the production in the wellfield. Tracer concentration profiles from repeated production-injection well doublets are fitted by two response curves representing both a low impedance fracture-dominated pathway and higher-impedance matrix-dominated pathway. Tracer curves are inverted for velocity, dispersion and swept area to compare changes in fluid pathways over time. Results from both wellfields suggest a net increase in fluid velocity and corresponding decrease in area swept for both fracture and matrix-dominated flowpaths. We also observe a small shift in percentage of tracer returns (injectate) towards fractures, corresponding with an increase in dispersivity, suggesting the utilization of more tortuous pathways through damage zones. Conversely, we see a decrease in dispersivity within the matrix reinforcing the idea of fluid focusing into lower impedance pathways. Overall, the wellfields in this study exhibit very high permeability and therefore do not mirror fracture evolution witnessed during pressure stimulation of very low permeability systems such as increased aperture or surface area. The results of this study highlight the importance of repeated tracer analysis when used to calibrate numerical models and long-term reservoir predictions.

1. INTRODUCTION

Geothermal operators routinely implement tracers test as a matter of defining reservoir characteristics, calibration of 3D numerical models and optimizing injection configurations. Developers often conduct testing at early stages to assist with resource capacity estimations, followed by continued testing throughout the lifetime of the wellfield. We compare tracer results from two fracture-dominated reservoirs in Eastern Nevada at times shortly following commissioning and again several years later. The results suggest changes in reservoir fracture permeability after only a few years of operation. Understanding how these changes translate to fracture geometry, retention time and speed of thermal breakthrough are important for projecting the results of early reservoir testing to later-stage operational conditions.

2. BACKGROUND

Ormat conducted reservoir tracer studies at two recently commissioned geothermal binary plants in Eastern Nevada, Don A. Campbell and McGinness Hills. The McGinness Hills (MGH) plant, located near Austen Nevada, began operation in May 2012 with production of 2750 ton/hr of brine with 100% reinjection (Norquist and Delwiche, 2013). A tracer study including 4 production and 2 injection wells, was commissioned in February 2013 utilizing two thermally stable naphthalene sulfonate tracers. Following the successful operation of MGH Phase I, an expansion to double power generation was commissioned in February 2015 producing a combined total of 7500 ton/hr. A second tracer study began in August 2015 following start-up and stabilization of the field. Highly permeable feedzones in the production and injection wells at MGH are hosted in competent/brittle monzonite and quartzite formations and correspond with a fracture network associated with a series of NNE-striking faults. While there is very little porespace in the crystalline bedrock to speak of, we find these to be extremely shattered units with interconnected fractures providing significant storage to the reservoir.

The Don A Campbell (DAC) plant, located near Gabbs Valley, NV, started generation in December 2013 with 4000 ton/hr production (Orenstein and Delwiche, 2014). Ormat conducted the first reservoir-wide tracer study at DAC in February 2014 utilizing 4 producers and 4 injectors. A second phase of power generation began operations in September 2015, producing a total of 8000 ton/hr with 100% reinjection. A follow-up tracer study began shortly thereafter in March 2016. DAC production and injection wells have feedzones hosted in thick silica-cemented alluvial sediments which are fractured along a series of NE-striking faults and overlay Tertiary volcanic bedrock. New MGH and DAC production and injection wells were included in subsequent tracer studies; however, we made an effort to repeat previously tested well doublets in attempts to characterize changes in injection pathways over time.

Tracer studies were conducted using unique naphthalene sulfonate tracers, each considered thermally stable at the low-to-moderate resource temperatures in both fields (<165ºC) (Rose et al, 2001). Tracers were injected as fast as possible with minimal disturbance to the injection pattern in order simulate a spike concentration of tracer at time zero. Cooled brine samples were collected at each production well and analyzed by HPLC and fluorimeter by the Energy & Geoscience Institute at the University of Utah, with detection limits as low as 0.05ug/kg for the various tracers.

Tracer results are treated here as concentration (µg/kg) versus time. Background, contamination and effects of recycling were removed from the dataset prior to analysis. Hydraulic properties of the tracer pathways were estimated from the tracer response curve using the advection-dispersion equation of solute transport (Horne et al, 1985 and references within). For one dimensional flow and instantaneous injection of tracer at time zero, the concentration at time *t* can be solved by:

$$C = \frac{s}{2}\sqrt{\frac{Pet_c}{\pi t}e^{\frac{Pe(t-t_c)^2}{4tt_c}}}$$

where *s* is the mass injected (kg), *Pe* is the Peclet number and t_c is the peak arrival time (s). The Dispersion coefficient, *D* (m^2/s), is given by *Pe=ux/D*, where *u* is the average fluid velocity (m/s) and *x* is the distance (m). We solve for longitudinal dispersivity α_L (m) from $D = \alpha u$ and the area swept along the pathway from $u=q/\rho A\varphi$ where φ is porosity of the flow channel, *A* is the height*width of the pathway (m^2), ρ is the water density (kg/m^3) and *q* is the injection rate (kg/s). Tracer return profiles were simulated with 2 or fewer response curves, and the properties of the response curves, fitted with a least-squares method. The program TRINV (Axellson et al, 2005) was used to optimize tracer curve inversions of *u, D* and $A\varphi$ using our initial fit. An example of a two-pulse fit is found below in Figure 1. Each example included in this study met a residual fit of 97% or better to 2 curves.

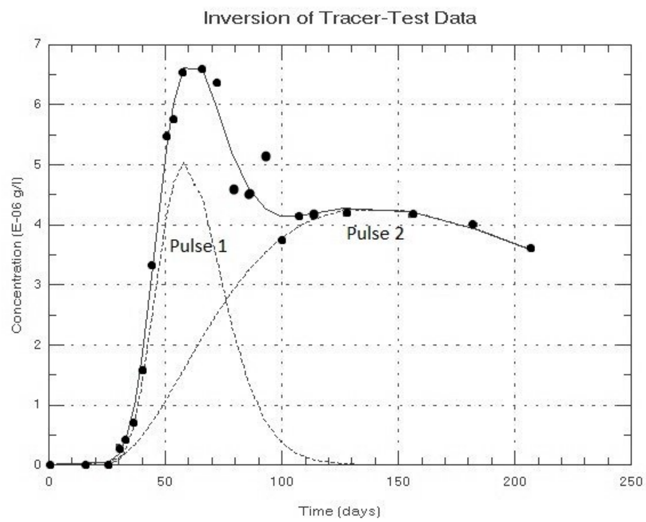

Figure 1: Example of 2-pulse curve fitting to MGH tracer response curve using the inverse model TRINV (Axellson et al, 2005) for solving flow parameters in both pulses. Two-pulse curves fit raw data within 98% in above example.

Fluid injection and production rates remained consistent over time in each production and injection well included in this study, which allowed for representative comparisons in flow parameters between well doublets. An exception to this was the DAC 26-6 injection well, which included a second high permeable well on its pad during the expansion of the plant in 2014. This effectively doubled injection into a similar feedzone and may have increased flow along the same pathway. We note the increase in total flow between earlier and later tracer studies as a mechanism for changes in individual fluid pathways.

3. RESULTS AND INTERPRETATION

Tracer return curves for repeated well tests are found in Figure 2. Tracer returns at both wellfields may be described as having multiple low impedance first peaks likely associated with fracture-dominated pathways, superimposed upon a larger, higher impedance pathway, likely associated with matrix permeability. Despite multiple peaks occurring in the data, we believe the results accurately reflect the reservoir conditions and are not the effect of sampling errors since we see similar patterns repeated from earlier to later testing. For the purposes of this study, we were able to fit each concentration profile with (1) one dominant or aggregate low-impedance pulse and (2) a second, larger, higher-impedance pulse. The flow parameters derived from both pulses in each well doublets are found below in Table 1.

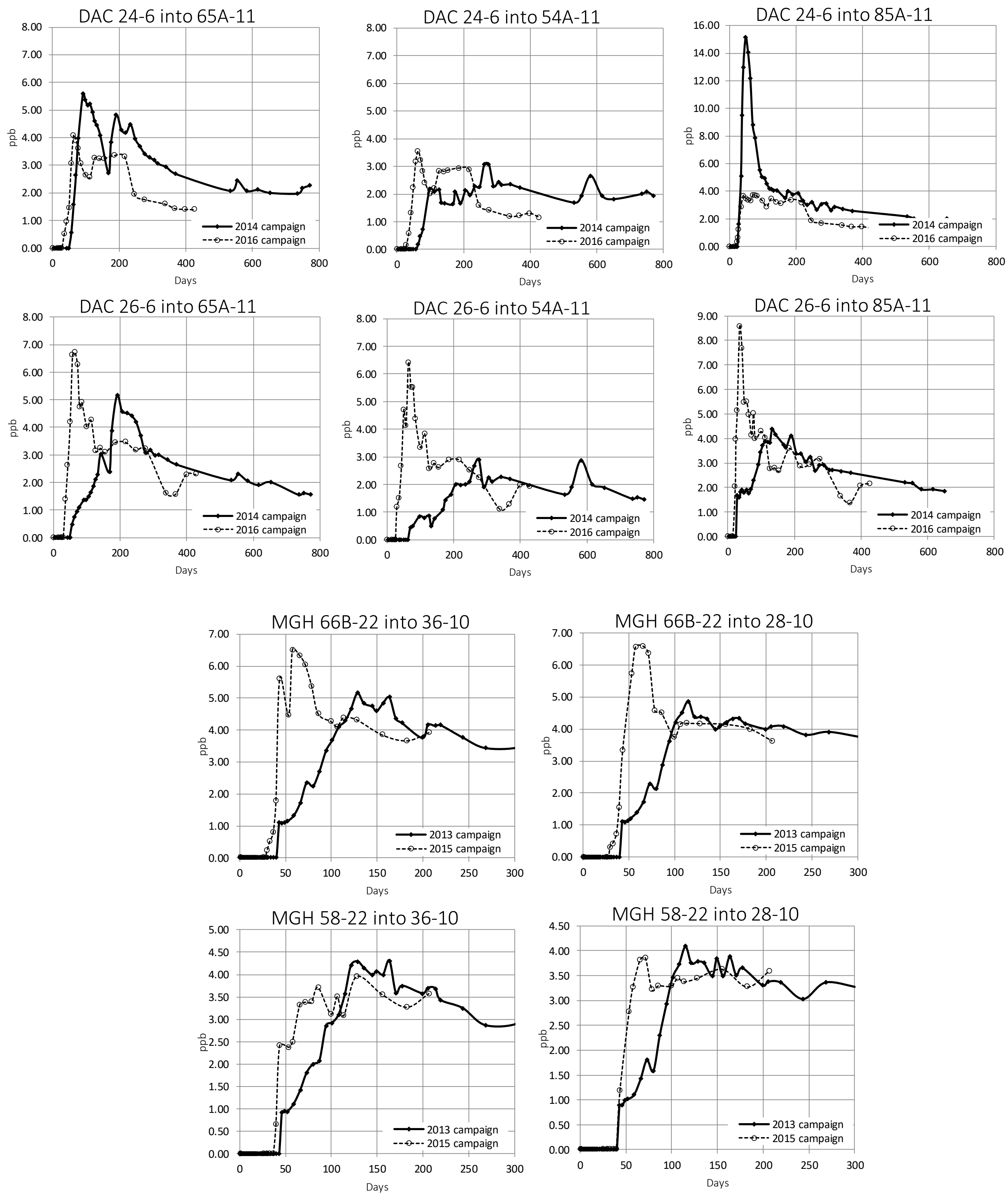

Figure 2: Tracer concentration response curves for three production and two injection wells at DAC (6 doublets) and two production wells and two injection wells at MGH (4 doublets), including data from both earlier and later tracer campaigns.

Table 1: Hydraulic parameters of flow pathways for DAC and MGH well doublets using tracer response curves.

				Pulse 1					**Pulse 2**						**Ratio of Mass**
Well-field	Producer	Injector	Year	*u* (m/s)	D (m2/s)	X-sect Area (m2)	αL (m)	Mass return(%)	*u* (m/s)	D (m2/s)	X-sect Area (m2)	αL (m)	Mass return(%)	Total Mass%	Pulse 1 : Pulse 2
DAC	65A-11	26-6	2014	1.5E-04	0.004	3227	28	4.1	8.3E-05	0.097	5839	1159	64.5	69	6 : 94
DAC	65A-11	26-6	2016	5.1E-04	0.050	956	97	5.6	1.5E-04	0.131	3250	875	37.8	43	13 : 87
DAC	65A-11	24-6	2014	3.6E-04	0.037	1369	103	8.7	1.4E-04	0.042	3438	297	30.2	39	
DAC	65A-11	24-6	2016	5.2E-04	0.039	932	74	3.4	1.9E-04	0.076	2604	407	21.6	25	
DAC	54-11	26-6	2014	3.4E-04	0.015	1410	45	0.8	8.8E-05	0.038	5515	431	31.4	32	16 : 90
DAC	54-11	26-6	2016	4.4E-04	0.100	1104	226	10.9	1.4E-04	0.029	3383	200	16.1	27	40 : 60
DAC	54-11	24-6	2014	3.3E-04	0.022	1473	67	2.7	9.8E-05	0.055	4989	559	35.8	39	7 : 93
DAC	54-11	24-6	2016	5.5E-04	0.058	888	106	3.7	1.9E-04	0.058	2564	303	16.4	20	18 : 82
MGH	28-10	66B-22	2013	3.8E-04	0.009	947	24	0.6	1.7E-04	0.224	2157	1335	33.8	34	2 : 98
MGH	28-10	66B-22	2015	7.0E-04	0.072	516	102	2.9	2.4E-04	0.200	1489	822	19.4	22	13 : 87
MGH	28-10	58-22	2013	4.1E-04	0.013	475	31	0.5	1.8E-04	0.261	1077	1441	29.0	30	2 : 98
MGH	28-10	58-22	2015	7.3E-04	0.068	266	93	1.6	2.9E-04	0.149	673	514	11.0	13	13 : 87
MGH	36-10	66B-22	2013	3.5E-04	0.024	1038	68	1.0	1.9E-04	0.268	1899	1401	31.3	32	3 : 97
MGH	36-10	66B-22	2015	7.6E-04	0.006	477	8	0.4	4.8E-04	0.306	767	642	12.0	12	4 : 96
MGH	36-10	58-22	2013						2.6E-04	0.214	754	826	18.6	19	
MGH	36-10	58-22	2013						3.9E-04	0.311	503	802	11.7	12	

Wells sampled during the second campaign overwhelmingly occur with faster first returns upwards of 22 days at DAC down from an average of 50 days, and 25 days at MGH down from an average of 40 days. For all well pairs at both MGH and DAC, the inverted average velocity increased in both pulses from the early to later tracer campaigns (Figure 3). Due to the relationship between area and velocity, we see a corresponding decrease in area swept for all pathways. This trend results in unique slopes with later-matrix pathways converging on top of early-fracture pathways for both DAC and MGH. Plots of velocity vs area for MGH suggest at least 2 unique pathways controlling flow through our set of well doublets. This overall trend correlates with a notable shift in total tracer mass returned from pulse 2 towards pulse 1 (Figure 4). Calculated dispersivity (αL), however, increases for all first pulses or fracture-dominated pathways, while second pulses or matrix-dominated pathways witnessed a decrease in dispersivity (Figure 3).

To explain the trends described above, we might envision a focusing-effect occurring because of prolonged injection, compounded with enhanced fracturing in the least-principle stress direction due to thermal contraction. As total flow is increased along predominant injection pathways, more fluid is focused from the matrix to the fractures resulting in high velocities, lower swept area and decreased dispersivity in the matrix. However, thermal contraction along these cooling pathways might lead to a decrease in faulted or fracture apertures, but an increase in fracture networks throughout the faulted damage zone explaining the observed increase in fracture dispersivity.

This phenomenon may be unique to extremely high permeability reservoirs where a ‘path of least-resistance’ is available for the injected fluids to choose between. In the case of low-to-moderate injectivity, namely within EGS stimulation studies, we find that high stimulating pressure within the reservoir assists in opening new pathways and fracture networks, typically increasing the available cross-sectional area for fluid movement (Rose et al, 2017; Lutz et al, 2010;Kwakwa, 1988). Dilation of faults, as found in stimulation studies, is an unlikely mechanism here as this would lead to a net decrease in dispersivity along fractures. Both DAC and MGH wellfields operate under minimal or zero injection wellhead pressure suggesting an excess of conductive matrix and fracture space for fluid to migrate. An established hydraulic pressure gradient is likely to build over time between injection and production in response to high volume exploitation, allowing for preferred movement in lower impedance pathways.

The exception to the above trend includes DAC injection well 26-6, where we find low impedance first-pulses occurring only during the second tracer campaign only (Figure 2). This change may be in response to a sudden increase in injection from the 26-series of new wells following the same flow path thus migrating towards new fracture-dominated conduits.

Major faults and fracture networks in MGH might be characterized as discrete large aperture planar features that are interconnected and deeply seated, while those at DAC better resemble a network of variably oriented fractures in a silicified damage zones between synthetic faults. MGH injection appears to have undergone a greater increase in velocity and greater decrease in cross-sectional area along fractured pathways for the same increase in dispersivity, possibly suggesting transverse spreading over broad, planar features. DAC tracer profiles suggest possible focusing of injection along established fracture conduits with similar depth and width and porosity.

Even after continued injection, the higher impedance matrix still represent a significant percentage of the total flow and surface area for both fields, typically greater than 87% (Figure 3). Reservoir lithologies may also play a significant role in how hydraulic properties in this matrix change over time. The larger surface area and lower dispersion coefficients at DAC correlate well with the highly porous alluvium, compared to the dense but shattered quartzite and monzonite units at MGH. In time, the porosity of units may change by formation of authigenic clay/hydrothermal mineralization and/or dissolution of cement, thus reducing surface area and forcing flow towards dominant fractures. In a cleanly fractured quartzite, mineralization along hydraulic pathways is still relevant, however more interconnected space remains along planar conduits for injection to flow. In the case of Ormat’s Eastern NV wellfields, continued injection is likely encouraging flow away from porous pathways and into networks of fractured media. The impact these trends have on long-term heat-mining within the reservoir is the topic of ongoing investigation.

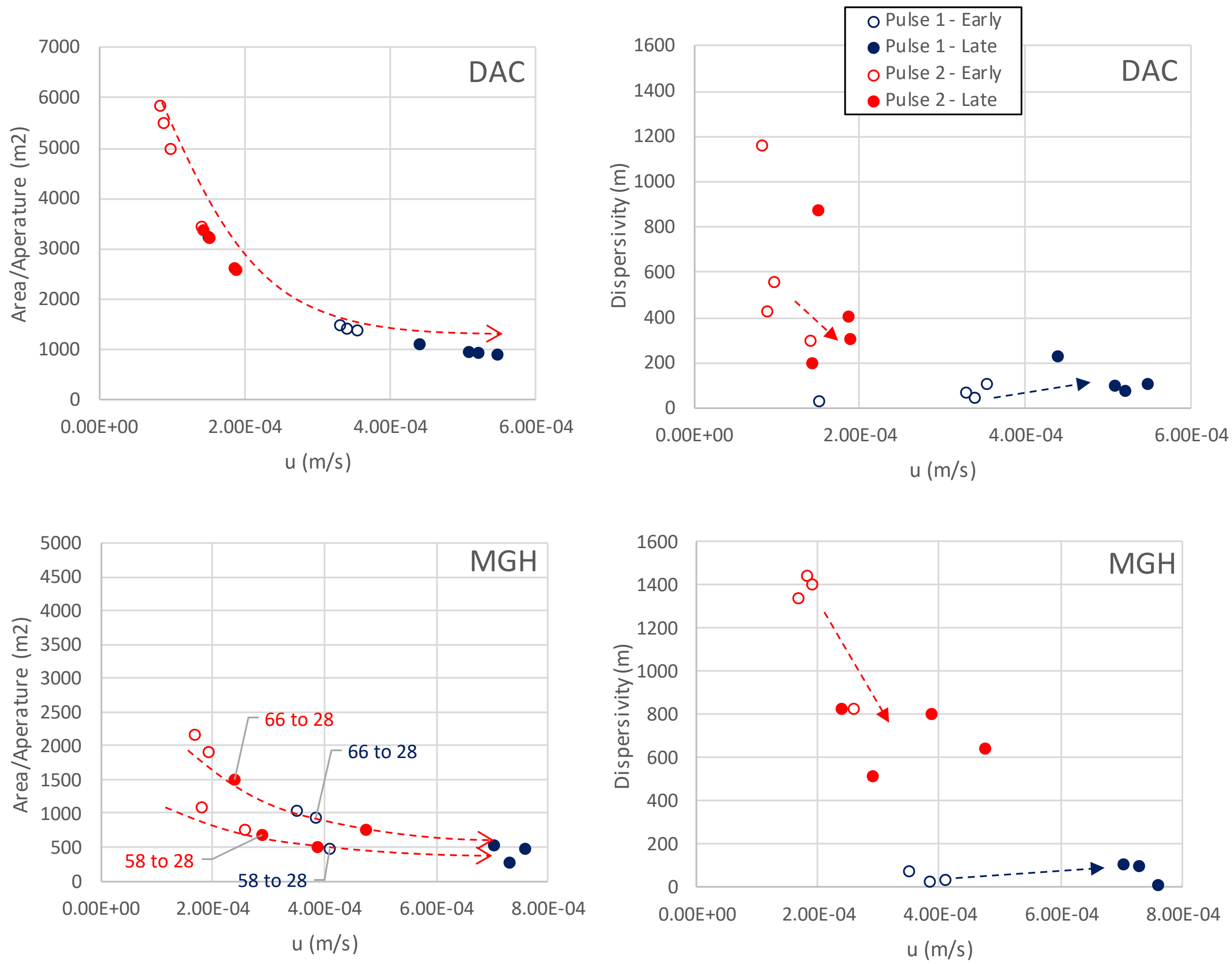

Figure 3: Left: Plots mean velocity (*u*) versus of area swept (*Aφ*) for both Pulse 1 and Pulse 2 at early and late time. Example well doublets in MGH highlighted demonstrating late matrix pathways overlapping with early-time fracture pathways. Right: Plots of mean velocity (u) and longitudinal dispersivity (α_L).

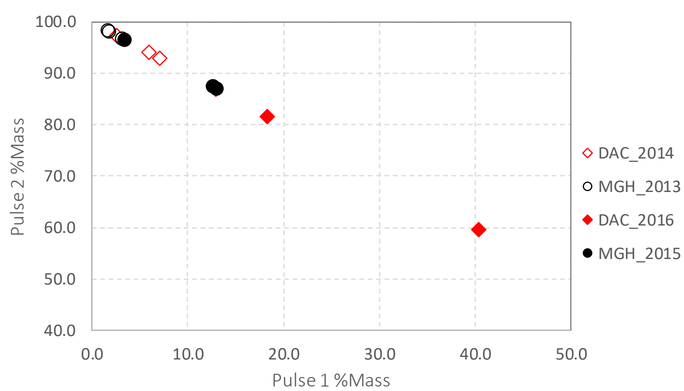

Figure 4: Plot of tracer mass shift in Pulse 2 (% mass of the total recovered in the well doublet) to Pulse 1 over both sampling campaigns

4. CONCLUSIONS

Tracer testing at both early and later times following plant start up result in variable tracer response curves between repeated well doublets. Investigation into the precise changes in hydraulic properties of the tracer pathways occurring over time lead to the following conclusions:

(1) For a highly permeable reservoir, the ratio of recovered tracer shifts from the second pulse to the first pulse, representing a preference in flow towards open, low impedance fracture pathways over time. Its important to note, however, that lower impedance matrix still represents the greater percentage of mass returns even after continued injection.

(2) Fluid velocities increase in both fracture dominated pathways and matrix dominated pathways over time resulting from lowered impedance in the fluid pathways, an increase in total production, or both.

(3) Faulted pathways evolve towards increased dispersivity and a lower combined surface area (φ * fracture width * height) over time. This is likely due to expanded movement through damage zones surrounding the planar structures and expansion of flow to greater depths and widths along those same planar pathways. Conversely, matrix pathways evolve towards having lower surface area and lower dispersivity, possibly due to movement of fluid from porespace to nearby fracture networks as a preferred, lower impedance method of transport.

(4) The decrease in effective cross-sectional area swept for both fracture and matrix pathways may be unique to very high permeability systems allowing for preferential flow or "drainage" towards lower impedance pathways.

(5) Results of tracer studies conducted shortly after well testing or plant start up may change following several months or years of production. Likewise, the heat transfer predictions based on early results may need to be updated with later tracer studies to account for these changes in hydraulic pathways. Sensitivity analyses to these thermal predictions is the subject of ongoing work.

REFERENCES

Axellson, G., Bjornsson, G. and Montalvo, F. 2005, Quantitative Interpretation of Tracer Test Data. Proceedings World Geothermal Congress April 2005.

Horne, R.N., Gilardi, J and Bouett, L. 1985, Dispersion of Tracers in Fractures – Experiments at Stanford University. Proceedings of 7th NZ Geothermal Workshop.

Kwakwa, K.A. 1988, Tracer Measurements during Long Term circulation of the Rosemanowes HDR Geothermal system. PROCEEDINGS, Thirteenth Workshop on Geothermal Reservoir Engineering Stanford university, Stanford, California, January 19-21, 1988 SGP-TR-113.

Lutz, S.J., Hickman, S., Davatzes, N., Zemach, E., Drakos, P. 2010, Rock Mechanical testing and Petrologic analysis in support of Well Stimulation activities at the Desert Peak geothermal field, Nevada. PROCEEDINGS, Thirty-Fifth Workshop on Geothermal Reservoir Engineering Stanford University.

Nordquist, J. and Delwiche ,B., 2013, The McGinness Hills Geothermal Project, GRC Transactions, Vol. 37

Orenstein, R. and Delwiche, B., 2014, The Don A. Campbell Geothermal Project, GRC Transactions, Vol 38

Rose, P.E., Benoit, W.R. and Kilbourne, P.M, 2001, The application of polyaromatic sulfonates as tracers in geothermal reservoirs. Geothermics, 30, 317-640.

Rose,P.R., Moore, J.M., Bradford,J., Mella,M., Ayling B and McLennan, J. 2017. Tracer Testing to Characterize Hydraulic Stimulation Experiments at the Raft River EGS Demonstration Site, GRC Transactions, Vol. 41.